IEICE TRANS. COMMUN., VOL.E105–B, NO.10 OCTOBER 2022

PAPER

Adaptive Resource Allocation Based on Factor Graphs in Non-Orthogonal Multiple Access

Taichi YAMAGAMI[†], ***Nonmember***, **Satoshi DENNO**[†a)], ***Senior Member***, ***and*** **Yafei HOU**[†], ***Member***

SUMMARY In this paper, we propose a non-orthogonal multiple access with adaptive resource allocation. The proposed non-orthogonal multiple access assigns multiple frequency resources for each device to send packets. Even if the number of devices is more than that of the available frequency resources, the proposed non-orthogonal access allows all the devices to transmit their packets simultaneously for high capacity massive machine-type communications (mMTC). Furthermore, this paper proposes adaptive resource allocation algorithms based on factor graphs that adaptively allocate the frequency resources to the devices for improvement of the transmission performances. This paper proposes two allocation algorithms for the proposed non-orthogonal multiple access. This paper shows that the proposed non-orthogonal multiple access achieves superior transmission performance when the number of the devices is 50% greater than the amount of the resource, i.e., the overloading ratio of 1.5, even without the adaptive resource allocation. The adaptive resource allocation enables the proposed non-orthogonal access to attain a gain of about 5 dB at the BER of 10^{-4}.

key words: *non-orthogonal multiple access, message passing algorithm, factor graphs, log-likelihood ratio*

1. Introduction

Machine-type communications (MTC) have been identified as a part of the fifth generation mobile communication system and the beyond 5th generation system for the society with Internet of things (IoT). The society with the IoT needs a lot of sensor devices with wireless communication functionality, which are going to be scattered around us. Massive connectivity is demanded to provide connection with those devices when the number of those devices grows extremely high. In a word, network capacity has to be increased for such massive MTC (mMTC), though amount of data sent by a device might not be huge. Many techniques have been proposed for enhancing the wireless network capacity. For instance, multi-user multiple input multiple output (MU-MIMO) [1] and orthogonal frequency division multiple access (OFDMA) [2], that are classified into orthogonal multiple access, have been investigated. Non-orthogonal multiple access also has been considered, because non-orthogonal multiple access potentially achieves higher capacity than orthogonal multiple access. Non-orthogonal multiple access (NOMA) [3]–[9], low-density signature (LDS) [10], [11], and sparse code multiple access (SCMA) [14], [15] have been proposed as non-orthogonal multiple access techniques. The power-domain NOMAs achieve superior performance with taking advantage of the terminal locations where the one terminal is far from the other terminal near by the base station, even though the complexity of the system is fairly small. While the power-domain NOMAs degrade in the situation where the terminals are located at similar distance from the base station, resource allocation techniques have been investigated [12], [13]. SCMAs and LDSs achieve superior performance even in the situation.

In this paper, we propose a non-orthogonal multiple access with adaptive resource allocation based on factor graphs. In the proposed non-orthogonal multiple access, multiple subcarriers in a resource block for a user are allocated to every device. Even if the number of the devices of the user is more than that of the subcarriers, the proposed non-orthogonal multiple access allows all the devices to transmit their packets simultaneously for high capacity mMTC. The message passing algorithm (MPA) [16], [17] is employed at the receiver side to detect the signal of all the devices. Furthermore, the proposed non-orthogonal multiple access applies adaptive resource allocation based on factor graphs that adaptively allocates the frequency resources to the devices for improvement of the transmission performances. This paper proposes two allocation algorithms for the proposed non-orthogonal multiple access.

2. System Model

2.1 Non-Orthogonal Multiple Access in Frequency Domain

We assume that one user has L devices to collect some information such as sensing data, by means of a wireless communication for IoT applications. The transmitter on the device sends the packets to the receiver on the base station. Only one antenna is installed on every device and the base station. Since only one resource block (RB) is allocated to a user, the devices communicates the base station with the limited number of the subcarriers in the RB. Figure 1 illustrates the RB allocation in a frequency band. Different frequency resources such as subcarriers are allocated to each device, and the devices transmit their packets on the allocated subcarriers. N_{S} subcarriers are allocated in an RB, while N_{F} subcarriers are available for the wireless communication. This means that $N_{\mathrm{F}}/N_{\mathrm{S}}$ RBs are available in the frequency band. We assume that the number of the devices owned by a

Manuscript received December 22, 2021.
Manuscript revised March 17, 2022.
Manuscript publicized April 15, 2022.

[†]The authors are with Graduate School of Natural Science and Technology, Okayama University, Okayama-shi, 700-8530 Japan.
a) E-mail: denno@okayama-u.ac.jp

DOI: 10.1587/transcom.2021EBP3213

Copyright © 2022 The Institute of Electronics, Information and Communication Engineers

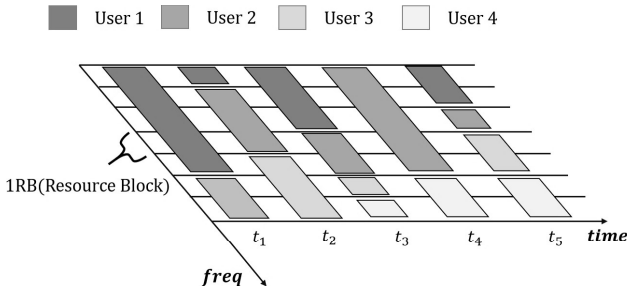

Fig. 1 Resource allocation in frequency domain.

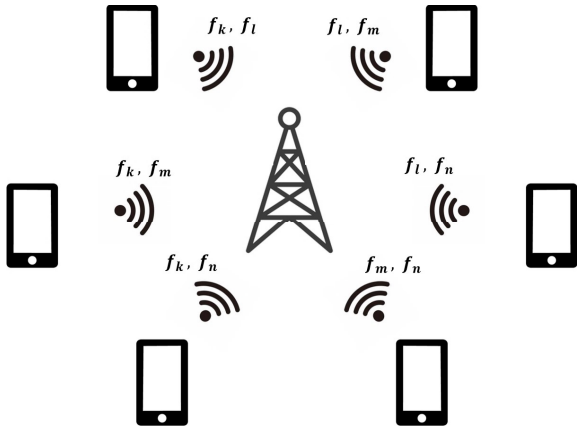

Fig. 2 Non-orthogonal multiple access.

user is more than that of the subcarriers allocated to the user, i.e., $L \geq N_\mathrm{s}$. When the user has all own devices transmit their packets simultaneously, the non-orthogonal access is used for the communication between the base station and the devices via one RB allocated to the user. We assume that the base station has a functionality to select the subcarriers within the given RB for a user. Figure 2 draws a non-orthogonal multiple access where the devices owned by the user transmit their packets to the base station via the allocated subcarriers in the RB. In the figure, f_k represents a frequency of a subcarrier in the RB allocated to a user.

Let $B = \{b(0), b(1), \cdots, b(N_\mathrm{s}-1)\}$ denote a set of subcarrier numbers in an RB assigned to a user, and its element $b(m) \in \mathbb{R}$ indicates an mth subcarrier number allocated to the user. Let $\boldsymbol{S}_l \in \mathbb{C}^{N_\mathrm{F}}$ denote a transmission signal vector for an lth device, the transmission signal vector can be defined with the inverse discrete Fourier transform (IDFT).

$$\boldsymbol{S}_l = \dot{\boldsymbol{F}}^\mathrm{H} \boldsymbol{X}_l \tag{1}$$

In (1), superscript H, $\boldsymbol{X}_l \in \mathbb{C}^{N_\mathrm{s}}$, and $\dot{\boldsymbol{F}} \in \mathbb{C}^{N_\mathrm{s} \times N_\mathrm{F}}$ represent Hermitian transpose of a vector, a modulation signal vector sent from the lth device, and a partial discrete Fourier transform matrix. Let j and $F_{n,m} \in \mathbb{C}$ represent the imaginary unit and an (n,m) element of the DFT matrix defined as,

$$F_{n,m} = \frac{1}{\sqrt{N_\mathrm{F}}} e^{-\mathrm{j}\frac{2\pi nm}{N_\mathrm{F}}}, \tag{2}$$

the partial discrete Fourier transform matrix is defined as follows.

$$\dot{\boldsymbol{F}} = \begin{pmatrix} F_{b(0),0} & F_{b(0),1} & \cdots & F_{b(0),N_\mathrm{F}-1} \\ F_{b(1),0} & F_{b(1),1} & \cdots & \vdots \\ \vdots & \cdots & \ddots & \vdots \\ F_{b(N_\mathrm{s}-1),0} & \cdots & \cdots & F_{b(N_\mathrm{s}-1),N_\mathrm{F}-1} \end{pmatrix} \tag{3}$$

All the devices simultaneously send their packets for the base station after the cyclic prefixes are added to those signals. The base station receives those transmission signals that have passed through multipath fading channels. If the channel length in the multipath fading channels is less than the cyclic prefix length, the channel matrix becomes circular. Let $\boldsymbol{H}_l \in \mathbb{C}^{N_\mathrm{F} \times N_\mathrm{F}}$ denote a circular channel matrix between the lth device and the base station, a received signal vector $\boldsymbol{Y} \in \mathbb{C}^{N_\mathrm{F}}$ in the time domain can be written as,

$$\boldsymbol{Y} = \sum_{l=1}^{L} \boldsymbol{H}_l \boldsymbol{S}_l + \boldsymbol{N}. \tag{4}$$

In (4), $L \in \mathbb{N}$ and $\boldsymbol{N} \in \mathbb{C}^{N_\mathrm{F}}$ represent the number of the devices owned by the user and an additive white Gaussian noise (AWGN) vector. If the received signal vector in the time domain is transformed into the frequency domain with the DFT, the vector in the frequency domain $\dot{\boldsymbol{Y}} \in \mathbb{C}^{N_\mathrm{s}}$ can be written as follows.

$$\begin{aligned} \dot{\boldsymbol{Y}} &= \dot{\boldsymbol{F}}\boldsymbol{Y} = \sum_{l=1}^{L} \dot{\boldsymbol{F}}\boldsymbol{H}_l\boldsymbol{S}_l + \dot{\boldsymbol{F}}\boldsymbol{N} \\ &= \sum_{l=1}^{L} \dot{\boldsymbol{F}}\boldsymbol{H}_l\dot{\boldsymbol{F}}^\mathrm{H}\boldsymbol{X}_l + \dot{\boldsymbol{F}}\boldsymbol{N} \\ &= \sum_{l=1}^{L} \boldsymbol{\Gamma}_l\boldsymbol{X}_l + \dot{\boldsymbol{F}}\boldsymbol{N} \end{aligned} \tag{5}$$

In (5), $\boldsymbol{\Gamma}_l \in \mathbb{C}^{N_\mathrm{s} \times N_\mathrm{s}}$ denotes a diagonal channel matrix with the frequency responses between the lth device and the base station in the diagonal positions, which is expressed as follows.

$$\boldsymbol{\Gamma}_l = \begin{pmatrix} \gamma_l(0) & & & 0 \\ & \gamma_l(1) & & \\ & & \ddots & \\ 0 & & & \gamma_l(N_\mathrm{s}-1) \end{pmatrix} \tag{6}$$

In (6), $\gamma_l(m)$ represents a frequency response in the mth subcarrier between the lth device and the base station, which is defined as,

$$\gamma_l(m) = \sum_{p=0}^{L_p-1} h_l(p) \exp\left(-\mathrm{j}2\pi\frac{mp}{N_F}\right), \tag{7}$$

where $L_p \in \mathbb{N}$ and $h_l(p) \in \mathbb{C}$ denote the number of the paths in the multipath fading channel and an impulse response of the pth path.

As is shown in (5), the received signal is superposition of the transmission signals from the L devices. If the

number of the superposed signals L increases, the transmission performance will be degraded, which might reduce the throughput in the non-orthogonal access. The following section proposes a technique to solve the problem of the throughput reduction caused by the transmission performance degradation.

3. Adaptive Resource Allocation in Non-Orthogonal Multiple Access

3.1 Non-Orthogonal Multiple Access with MPA

As is described before, the L devices transmit their packet via the subcarriers in the RB. While the RB consists of N_s subcarriers, M subcarriers are allocated to every device in the proposed non-orthogonal access where M is set as $N_\mathrm{s}/L < M \leq N_\mathrm{s}$. If all the devices simultaneously start the communication with the base station, the communication channel will get overloaded. Figure 3 illustrates an example of the subcarrier allocation to the devices when $M = 2$ and $N_\mathrm{s} = 4$, where every device transmits their packets via two subcarriers.

The information bit sequence is encoded and its output bits are provided to a modulator via an interleaver. The signals from the modulator are transmitted to the base station via the allocated subcarriers. Let $\boldsymbol{X}_{0,l} \in \mathbb{C}^{N_\mathrm{s}}$ denote a modulation signal vector for the lth device, the vector can be expressed as follows.

$$\boldsymbol{X}_{0,l} = \boldsymbol{C}_{0,l}\, x(l) \tag{8}$$

In (8), $x(l) \in \mathbb{C}$ and $\boldsymbol{C}_{0,l} \in \mathbb{R}^{N_\mathrm{s}}$ represent a modulation signal sent from the lth device and a subcarrier allocation vector defined as $\boldsymbol{C}_{0,l} = [c_{0,l}(0) \cdots c_{0,l}(N_\mathrm{s}-1)]^\mathrm{T}$, where superscript T and $c_{0,l}(m) \in \mathbb{R}$ indicate transpose of a vector and the mth element of the vector $\boldsymbol{C}_{0,l}$, which is defined as,

$$c_{0,l}(m) = \begin{cases} 1 & (m\,\text{th subcarrier is available}) \\ 0 & (m\,\text{th subcarrier is not available}) \end{cases} \tag{9}$$

As is shown in (8) and (9), the device actually only transmits the same packet in the M subcarriers. Let $\overline{\boldsymbol{C}_0} \in \mathbb{C}^{N_\mathrm{s}\times L}$ denote a subcarrier allocation matrix, the matrix is defined as $\overline{\boldsymbol{C}_0} = [\boldsymbol{C}_{0,1} \cdots \boldsymbol{C}_{0,L}]$. For example, when $N_\mathrm{s} = 4$ and $M = 2$, the subcarrier allocation matrix $\overline{\boldsymbol{C}_0}$ can be given as follows [14].

$$\begin{aligned} \overline{\boldsymbol{C}_0} &= [\boldsymbol{C}_{0,1} \cdots \boldsymbol{C}_{0,6}] \\ &= \begin{pmatrix} 1 & 1 & 1 & 0 & 0 & 0 \\ 1 & 0 & 0 & 1 & 1 & 0 \\ 0 & 1 & 0 & 1 & 0 & 1 \\ 0 & 0 & 1 & 0 & 1 & 1 \end{pmatrix} \end{aligned} \tag{10}$$

Figure 3 draws the non-orthogonal access with the subcarrier allocation matrix $\overline{\boldsymbol{C}_0}$.

When the transmission signal vector is defined in (8), the receive signal vector $\dot{\boldsymbol{Y}}_0$ can be rewritten as follows.

$$\begin{aligned} \dot{\boldsymbol{Y}}_0 &= \sum_{l=1}^{L} \boldsymbol{\Gamma}_l \boldsymbol{X}_l + \dot{\boldsymbol{F}}\boldsymbol{N} \\ &= \sum_{l=1}^{L} \boldsymbol{\Gamma}_l \boldsymbol{C}_{0,l}\, x(l) + \dot{\boldsymbol{F}}\boldsymbol{N} \\ &= \overline{\boldsymbol{\Gamma}_0}\dot{\boldsymbol{X}} + \dot{\boldsymbol{F}}\boldsymbol{N} \end{aligned} \tag{11}$$

In (11), $\dot{\boldsymbol{X}} \in \boldsymbol{C}^L$ and $\overline{\boldsymbol{\Gamma}_0} \in \boldsymbol{C}^{N_\mathrm{s}\times L}$ denote a combined transmission vector defined as $\dot{\boldsymbol{X}} = [x(1) \cdots\cdots x(L)]^\mathrm{T}$ and an equivalent channel matrix, which is defined as,

$$\overline{\boldsymbol{\Gamma}_0} = [\boldsymbol{\Gamma}_1 \boldsymbol{C}_{0,1} \cdots\cdots \boldsymbol{\Gamma}_L \boldsymbol{C}_{0,L}]. \tag{12}$$

When $N_\mathrm{s} = 4$ and $M = 2$, $\overline{\boldsymbol{\Gamma}_0}$ is expressed with frequency response $\gamma_l(m)$ in the following.

$$\begin{aligned} \overline{\boldsymbol{\Gamma}_0} &= [\boldsymbol{\Gamma}_1 \boldsymbol{C}_{0,1} \cdots\cdots \boldsymbol{\Gamma}_6 \boldsymbol{C}_{0,6}] \\ &= \left[\begin{pmatrix} \gamma_1(0) & & 0 \\ & \ddots & \\ 0 & & \gamma_1(3) \end{pmatrix} \begin{pmatrix} 1 \\ 1 \\ 0 \\ 0 \end{pmatrix} \cdots \right. \\ &\qquad \left. \cdots \begin{pmatrix} \gamma_6(0) & & 0 \\ & \ddots & \\ 0 & & \gamma_6(3) \end{pmatrix} \begin{pmatrix} 0 \\ 0 \\ 1 \\ 1 \end{pmatrix} \right] \\ &= \begin{pmatrix} \gamma_1(0) & \gamma_2(0) & \gamma_3(0) & 0 & 0 & 0 \\ \gamma_1(1) & 0 & 0 & \gamma_4(1) & \gamma_5(1) & 0 \\ 0 & \gamma_2(2) & 0 & \gamma_4(2) & 0 & \gamma_6(2) \\ 0 & 0 & \gamma_3(3) & 0 & \gamma_5(3) & \gamma_6(3) \end{pmatrix} \end{aligned} \tag{13}$$

The system model of the proposed non-orthogonal access defined in (11) can be described by a bipartite graph, which is regarded as a factor graph. Figure 4 illustrates a factor graph when the equivalent channel matrix $\overline{\boldsymbol{\Gamma}_0}$ is used, i.e., $M = 2$, $N_\mathrm{s} = 4$. As is shown in the figure, the upper nodes and the lower nodes are called variable nodes and observation nodes, respectively. Each variable node is connected to two observation nodes, and each observation node is connected to three variable nodes. This implies that three signals are received at one subcarrier. Figure 4 shows that the factor graph has the smallest cycle of 6 edges. If the smallest cycle is long enough, the message passing algorithm (MPA) can improve the detection performance. Since the MPA output

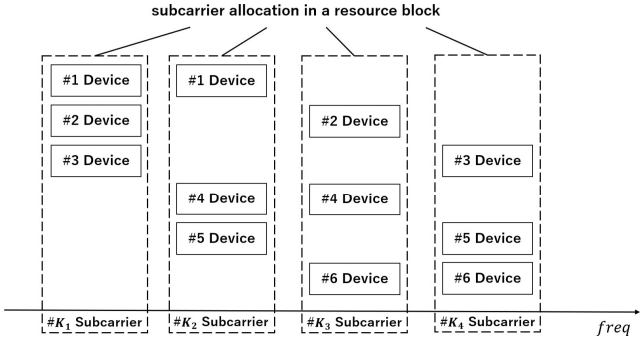

Fig. 3 Subcarrier allocation for devices.

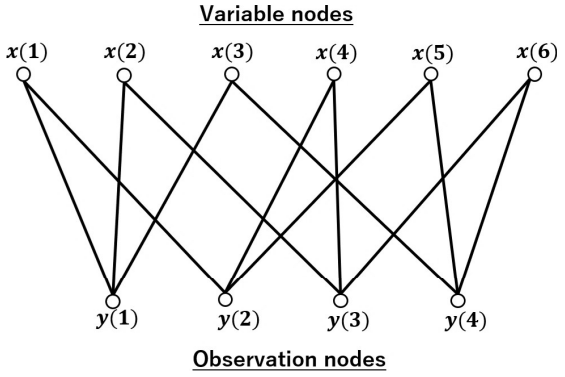

Fig. 4 Factor graph representation of non-orthogonal access.

signals contain all the signals, the MPA output signals are divided for the respective decoders dedicated to the devices.

Whereas the subcarrier allocation based on $\overline{\boldsymbol{C}_0}$ is used in Fig. 4, another subcarrier allocation can be considered instead of $\overline{\boldsymbol{C}_0}$. We propose a technique that adaptively selects the best subcarriers allocation among all the possible subcarrier allocations for enhancing the transmission performance. The detail of the proposed technique is described in the following sections.

3.2 Adaptive Resource Allocation

As is described previously, there are some possible subcarrier allocations other than $\overline{\boldsymbol{C}_0}$. Because the system model of the proposed non-orthogonal multiple access defined in (11) is dependent on not only the channel matrices $\boldsymbol{H}_l \ \ l = 1 \sim L$ but also the subcarrier allocation, even if the channel matrices do not change, the transmission performance of the proposed system might be improved by changing the subcarrier allocations. Because the subcarrier allocation is specified by the subcarrier allocation matrix, another subcarrier allocation can be formed with another subcarrier allocation matrix. Another subcarrier allocation can be given by permuting the columns in the subcarrier allocations matrix $\overline{\boldsymbol{C}_0}$. If the pth column is permuted with the qth column, this permutation can be described by the one-to-one mapping $(1\,2\cdots p\cdots q\cdots L) \rightarrow (1\,2\cdots q\cdots p\cdots L)$. Let this permutation be indexed by α, the one-to-one mapping is expressed with $(1\,2\cdots p\cdots q\cdots L) \xrightarrow{\alpha} (1\,2\cdots q\cdots p\cdots L)$ in this paper. If other subcarrier allocations can be given by the permutation, the number of the possible subcarrier allocations is $L! = \left(\begin{array}{c} L \\ 1 \end{array} \right)$. Another subcarrier allocation can be obtained by other technique. Therefore, the subcarrier allocation matrix generation based on the permutation might not be sufficient to get the optimum subcarrier allocation. In other words, the best subcarrier allocation might not be obtained by means of the permutation. However, we start with the permutation, because the permutation is easy to implement, which is suitable for the first step of our challenge. In addition, the permutation can keep the characteristics that an observation node is connected to three variable nodes and an variable node is connected to two variable nodes. Let $\boldsymbol{d}_l \in \mathbb{R}^{N_s}$ denote the lth column vector of subcarrier allocation matrix $\overline{\boldsymbol{C}_0}$, the matrix $\overline{\boldsymbol{C}_0}$ can be rewritten as,

$$\overline{\boldsymbol{C}_0} = [\ \boldsymbol{d}_1\ \boldsymbol{d}_2\ \cdots\ \boldsymbol{d}_L\ ]. \tag{14}$$

If the one-to-one mapping $(1\,2\cdots L) \xrightarrow{\alpha} (i_1\,i_2\cdots i_L)$ is applied to the subcarrier allocation matrix $\overline{\boldsymbol{C}_0}$, the subcarrier allocation matrix $\overline{\boldsymbol{C}_\alpha} \in \mathbb{R}^{N_s \times L}$ can be obtained as,

$$\begin{aligned} \overline{\boldsymbol{C}_\alpha} &= [\boldsymbol{d}_{i_1}\, \boldsymbol{d}_{i_2}\, \cdots\, \boldsymbol{d}_{i_L}] \\ &= [\boldsymbol{C}_{\alpha,1}\, \boldsymbol{C}_{\alpha,2}\, \cdots\, \boldsymbol{C}_{\alpha,L}] \end{aligned} \tag{15}$$

In (15), $\boldsymbol{C}_{\alpha,l} \in \mathbb{R}^{N_s}$ denotes an lth column of the subcarrier allocation matrix $\overline{\boldsymbol{C}_\alpha}$. When the subcarrier allocation matrix $\overline{\boldsymbol{C}_\alpha}$ is used, the equivalent channel matrix is changed to,

$$\overline{\boldsymbol{\Gamma}_\alpha} = [\boldsymbol{\Gamma}_0\boldsymbol{C}_{\alpha,0}\ \boldsymbol{\Gamma}_1\boldsymbol{C}_{\alpha,1}\ \cdots\cdots\ \boldsymbol{\Gamma}_{L-1}\boldsymbol{C}_{\alpha,L-1}]. \tag{16}$$

$\overline{\boldsymbol{\Gamma}_\alpha} \in \mathbb{C}^{N_s \times L}$ in (16) represents an equivalent channel matrix with the subcarrier allocation based on the mapping α. If the equivalent channel matrix is transformed from $\overline{\boldsymbol{\Gamma}_0}$ to $\overline{\boldsymbol{\Gamma}_\alpha}$, the system model defined in (11) is also rewritten as,

$$\dot{\boldsymbol{Y}}_\alpha = \overline{\boldsymbol{\Gamma}}_\alpha \dot{\boldsymbol{X}} + \dot{\boldsymbol{F}}\boldsymbol{N}. \tag{17}$$

In (17), $\dot{\boldsymbol{Y}}_\alpha \in \mathbb{C}^{N_s}$ represents a received signal vector when the subcarrier allocation with the matrix $\overline{\boldsymbol{C}_\alpha}$ is applied to the system. Let $\dot{\boldsymbol{Y}}_\alpha$ be defined as $\dot{\boldsymbol{Y}}_\alpha = [\dot{y}_\alpha(1), \dot{y}_\alpha(2), \cdots \dot{y}_\alpha(N_s)]^{\mathrm{T}}$ where $\dot{y}_\alpha(i) \in \mathbb{C}$ represents an ith received signal in the system, the received signal at the mth subcarrier $\dot{y}_\alpha(m)$ can be written as,

$$\dot{y}_\alpha(m) = \sum_{l \in D_{\alpha,m}} \gamma_l(m)x(l) + n(m). \tag{18}$$

In (18), $D_{\alpha,m}$ indicates a set that contains column numbers of non-zero elements in the mth row of the subcarrier allocation matrix $\overline{\boldsymbol{C}_\alpha}$. For example, $D_{0,1} = \{1, 2, 3\}$, because elements of "1" exist at 1st, 2nd, and 3rd columns in the 1st row of the matrix $\overline{\boldsymbol{C}_0}$ defined in (10). Because we assume that the proposed non-orthogonal multiple access is applied to the uplink, the devices send their packets via the subcarrier determined by the proposed subcarrier allocation. To implement the system, the base station carries out the channel estimation and selects the subcarrier allocation matrix with the estimated channel matrices. After that, the base station informs all the devices the subcarrier allocation in the down link prior to the uplink signal transmission. The devices do not need any channel state information in the proposed non-orthogonal access.

Next section proposes algorithms to select an appropriate subcarrier allocation matrix to achieve better transmission performance.

3.3 Algorithms for Adaptive Subcarrier Allocation

Because the MPA is utilized at the base station to detect all the transmission signals, the transmission performance is

characterized by the log-likelihood ratio (LLR). If the LLR can be estimated exactly at the base station, the transmission performance can be predicted. Since the transmission performance is dependent on the signal power to interference power ratio (SIR) in non-orthogonal multiple access systems, the LLR performance can be approximately estimated in the noise-free channel. This means that the transmission performance can be estimated at the base station even without the received signals, if the channel matrices are accurately estimated. Let $\boldsymbol{X}^{(\beta)} \in \mathbb{C}^L$ denote a βth candidate of the transmission signal vector, a received signal in the non-orthogonal noise-free channel with the subcarrier allocation matrix $\overline{\boldsymbol{C}_\alpha}$ is written as,

$$y_\alpha^{(\beta)}(m) = \sum_{l \in D_{\alpha,m}} \gamma_l(m) x^{(\beta)}(l). \tag{19}$$

In (19), $x^{(\beta)}(l) \in \mathbb{C}$ represents an lth element of the vector $\boldsymbol{X}^{(\beta)}$, i.e., $\boldsymbol{X}^{(\beta)} = [x^{(\beta)}(0) \cdots x^{(\beta)}(N_s - 1)]^{\mathrm{T}}$. The symbol LLR of the signal $x^{(\beta)}(l)$ can be obtained as follows.

$$\begin{aligned}
\Lambda_{\alpha,m}^{(\beta)}(x(l)=c) &= \log \frac{\mathrm{P}(x(l) = c \mid y_\alpha^{(\beta)}(m))}{\mathrm{P}(x(l) = \overline{c} \mid y_\alpha^{(\beta)}(m))} \\
&\approx \max_{x(l)=c} \left\{ -\frac{1}{2} |y_\alpha^{(\beta)}(m) - \overline{\boldsymbol{\Gamma}}_\alpha(m) \overline{\boldsymbol{X}}|^2 + \sum_{k \in B_{\alpha,m} \setminus l} \frac{\mathrm{P}(x(k))}{\mathrm{P}(x(k) = \overline{c})} \right\} \\
&\quad - \max_{x(l)=\overline{c}} \left\{ -\frac{1}{2} |y_\alpha^{(\beta)}(m) - \overline{\boldsymbol{\Gamma}}_\alpha(m) \overline{\boldsymbol{X}}|^2 + \sum_{k \in B_{\alpha,m} \setminus l} \frac{\mathrm{P}(x(k))}{\mathrm{P}(x(k) = \overline{c})} \right\} \\
&\quad + \log \frac{\mathrm{P}(x(l) = c)}{\mathrm{P}(x(l) = \overline{c})}
\end{aligned} \tag{20}$$

In (20), $\Lambda_{\alpha,m}^{(\beta)}(x(l)=c) \in \mathbb{R}$, $\mathrm{P}(a)$, $\mathrm{P}(A \mid B)$, $\overline{\boldsymbol{X}} \in \mathbb{C}^L$ and $\overline{c}$, represent a symbol LLR of the modulation signal $x(l) = c$, probability that an event a happens, conditional probability of an event A when an event B occurred, a tentative transmission signal vector, and a reference modulation signal, respectively. The same reference signal is used through the detection based on the MPA in spite of the signals $x^{(\beta)}(l)$. The MPA updates the LLRs based on (20) to improve the transmission performance. Actually, the MPA exchanges the extrinsic information on the factor graph. We can evaluate how accurately the MPA demodulates the signal vector by comparing the candidate vector $\boldsymbol{X}^{(\beta)}$ and the MPA output vector. To evaluate the accuracy of the MPA output vector, we introduce a metric called "reliability". For example, the reliability of the $l$the modulation signal is denoted as $\Delta\Lambda_{\alpha,m}^{(\beta)}(x(l)) \in \mathbb{R}$. Let $c_{\max}$ denote a modulation signal that maximizes the LLR among all the modulation signal candidates except for the transmission signal $x^{(\beta)}(l)$, the reliability of the lth modulation signal can be defined with the LLR as,

$$\begin{aligned}
\Delta\Lambda_{\alpha,m}^{(\beta)}(x(l)) &= -\Lambda_{\alpha,m}^{(\beta)}(x(l)=c_{\max}) + \Lambda_{\alpha,m}^{(\beta)}(x(l)=x^{(\beta)}(l)) \\
&= -\log \frac{\mathrm{P}(x(l) = c_{\max})}{\mathrm{P}(x(l) = \overline{c})} + \log \frac{\mathrm{P}(x(l) = x^{(\beta)}(l))}{\mathrm{P}(x(l) = \overline{c})} \\
&= \log \frac{\mathrm{P}(x(l) = x^{(\beta)}(l))}{\mathrm{P}(x(l) = c_{\max})}.
\end{aligned} \tag{21}$$

We propose to select the best subcarrier allocation matrix, i.e., the mapping, that maximizes the reliability $\Delta\Lambda_{\alpha,m}^{(\beta)}(x(l))$ for the optimum transmission performance in the non-orthogonal multiple access.

The following section propose two actual algorithms to maximize the reliability.

3.3.1 Maximization of Least Reliability (MLR)

Because the L devices transmit their packets simultaneously, the transmission performance is strongly affected by the other devices' performance. We have to evaluate the transmission performance on the assumption that any superpositions of the packets can be received at the base station. The average BER performance of all the devices is dominated by the worst device. The average BER performance is improved as the BER of the worst device gets better. We select the subcarrier allocation that maximizes the reliability of the worst device. In a word, we take the min-max approach. The reliability for the lth device $\Psi_\alpha^{(\beta)}(l) \in \mathbb{R}$ is calculated as,

$$\Psi_\alpha^{(\beta)}(l) = \left\langle \sum_{l \in D_{\alpha,m}} \Delta\Lambda_{\alpha,m}^{(\beta)}(x(l)) \right\rangle, \tag{22}$$

where $\langle \xi \rangle$ indicates the average of a variable ξ during a packet. The reliability for the lth device can be verified when all the possible candidates of the transmission signal vectors $\boldsymbol{X}^{(\beta)}$ are generated with equal probability.

$$\Psi_\alpha(l) = \frac{1}{Q^L} \sum_{\beta=0}^{Q^L-1} \Psi_\alpha^{(\beta)}(l) \tag{23}$$

In (23), $\Psi_\alpha(l) \in \mathbb{R}$ represents the reliability of the lth device when the mapping α is used for the subcarrier allocation, where Q denotes cardinally of a modulation scheme. For example, $Q = 4$, when the QPSK is used. We search the worst device that has the worst reliability in all the devices as,

$$l_{\min} = \arg\min_l \Psi_\alpha(l). \tag{24}$$

where $l_{\min}$ represents an index of the worst device. The proposed algorithm finds the subcarrier allocation that maximizes the reliability of the worst device $\Psi_\alpha(l_{\min})$ as follows.

$$\alpha_{\mathrm{MLR}} = \arg\max_\alpha \Psi_\alpha(l_{\min}) \tag{25}$$

α_{MLR} denotes an index of the subcarrier allocation selected by the proposed algorithm. The proposed algorithm is called "maximizing of least reliability (MLR)" in this paper.

3.3.2 Maximization of Averaged Reliability (MAR)

While the worst device in terms of the reliability is searched

by the MLR algorithm, the average BER performance of all the devices is desired to improve in wireless communication systems. We propose an algorithm that improves the average transmission performance. The proposed algorithm is called "maximizing of average reliability (MAR)" in this paper. The proposed MAR applies a reliability which is the average of all the devices' reliability $\Psi_{\alpha}^{(\beta)}(l)$, which is named as the average reliability. The reliability is defined in the following.

$$\overline{\Psi}_{\alpha} = \frac{1}{L}\sum_{l=0}^{L-1}\Psi_{\alpha}(l) \tag{26}$$

While the MLR takes the min-max approach, the MAR algorithm takes an average maximization approach as,

$$\alpha_{\mathrm{MAR}} = \arg\max_{\alpha}\overline{\Psi}_{\alpha}. \tag{27}$$

α_{MAR} represents an index selected by the MAR.

4. Computer Simulation

The BER performance of the proposed non-orthogonal multiple access is evaluated by computer simulation. The modulation scheme is quaternary phase shift keying (QPSK), and the half rate convolutional code with a constraint length of 3 is used. Multipath Rayleigh fading based on the Jakes' model is applied to the channels between the base station and the devices. All the channel gains between the antennas on the device and that on the base station are independent and identically distributed (i.i.d.). This means that the devices are located at the same distance from the base station. The performance of the proposed non-orthogonal access is evaluated in the situation where the power-domain NOMAs degrade severely. The number of the subcarriers N_{F} and that of the subcarriers in an RB N_{s} are 128 and 4, respectively. In addition, the number of devices L and that of the subcarrier allocated to a device M are set to 6 and 2, respectively. Table 1 summarizes the simulation parameters[†]. The performance of the fixed subcarrier allocation (FSA) is also evaluated as a reference, which is referred as the FSA in this paper[††]. The transmission power of the devices is kept constant in spite of access schemes.

[†]Since the system model is described in a low pass equivalent system as is defined in (4), all the channel gains are normalized by the transmission power in the low pass equivalent system. While the performance depends on the E_{b}/N_0, We do not explicitly define the transmission power and the channel gains in the low pass equivalent system when evaluating the transmission performance. When we design the system, we will have to set the transmission power taking account of the channel gains in the system. Such a system design including the definition of the transmission power is definitely one of our future works.

[††]When the FSA is applied to the proposed access, the same subcarriers are allocated to the devices despite of the channel gains. In a word, the FSA is a technique described only up to Sect. 3.1. Since the matrix defined in (10) is borrowed from literature where the SCMA is proposed [14], the proposed non-orthogonal access with the FSA is regarded as can be regarded as one configuration of the SCMA. Therefore, the performance comparison with the FSA is regarded as the performance comparison with one of the SCMAs.

Table 1 Simulation parameters.

Modulation scheme	QPSK / multicarrier
Channel code	Convolutional code
Coding rate & Constraint length	1/2&3
Decoding	Viterbi algorithm
Number of transmit antennas	1
Number of receive antennas	1
Number of devices	6
Number of FFT points	128
Number of subcarriers in a resource block	4
Channel model	Multipath fading
Number of MPA iterations	3

4.1 Reliability

The cumulative distribution function (CDF) of the reliability of the worst device $\Psi_{\alpha}(l_{\min})$ is shown in Fig. 5. In the figure, the CDF of the reliability $\Psi_{\alpha_{\mathrm{MLR}}}(l_{\min})$ with the subcarrier allocation based on the MLR is compared with that based on the FSA. 4 path-Rayleigh fading is used in the performance evaluation. The set of the RB $B = \{1, 2, 3, 4\}$ is applied in the figure. This figure shows that the MLR can increase the reliability, since the FSA has no functionality to increase the reliability. Figure 6 shows the CDF performance of the reliability $\overline{\Psi}_{\alpha}$ for the MAR. In the figure, the CDF of the average reliability with the adaptive subcarrier allocation based on the MAR is compared with that with the FSA. The channel model and the RB set are the same to those in Fig. 5. The figure shows that the MAR can increase the reliability. However, the reliability of the MAR can not be directly compared with that of the MLR, because the definition of the reliability of the MLR is different from that of the MAR[†††]. Instead of the reliability, we use the soft input signal fed to the decoder at the receiver for the performance measure of the two algorithms, the MLR and MAR. Figure 7 shows the CDF of the absolute value of the soft input signals fed to the decoder for the worst device. The channel model and the RB set are the same to those of Fig. 5 and Fig. 6. The $E_{\mathrm{b}}/N_0 = 20\,\mathrm{dB}$. The performances of the MLR, the MAR, and the FSA are compared in the figure. In addition, the performance of the OFDMA, a representative of orthogonal multiple access, is added as a reference. As is expected from the previous performance evaluation, the proposed adaptive resource allocation increases the absolute of the soft input signals, which infers that the proposed adaptive resource allocation achieves better transmission performance in the proposed non-orthogonal multiple access. Although the OFDMA produces the soft signals with the higher amplitude among all the access schemes, the OFDMA cannot suppress the probability that the small soft signals are fed to the channel decoder. The probability seems to be a little bit worse then that of the other schemes. The diversity gain can not be obtained in the OFDMA, because one subcarrier

[†††]When we consider that the proposed algorithm is implemented with fixed point digital signal processors, we should take account of the dynamic range in designing the hardware configuration. Such implementation issue is one of our future works.

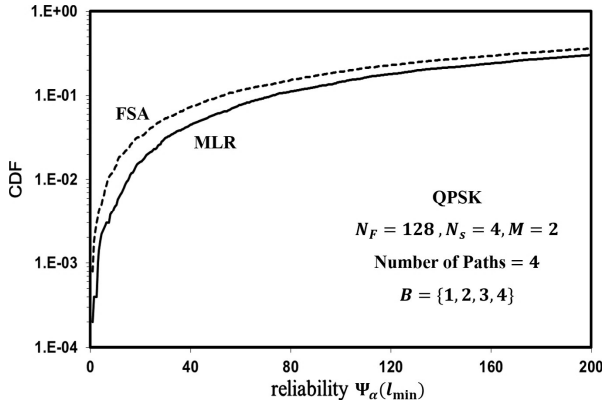

Fig. 5 CDF of reliability of worst device $\Psi_\alpha(l_{\min})$.

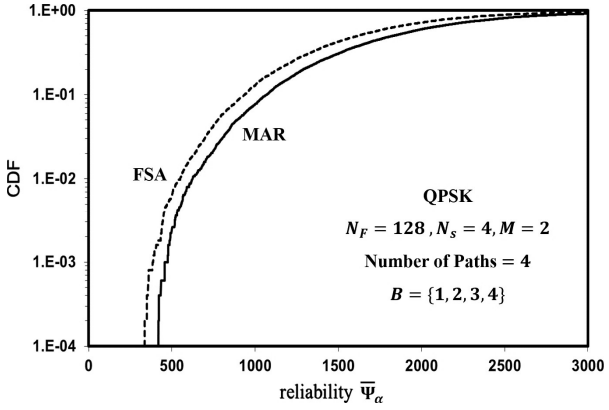

Fig. 6 CDF of average reliability $\overline{\Psi}_\alpha$.

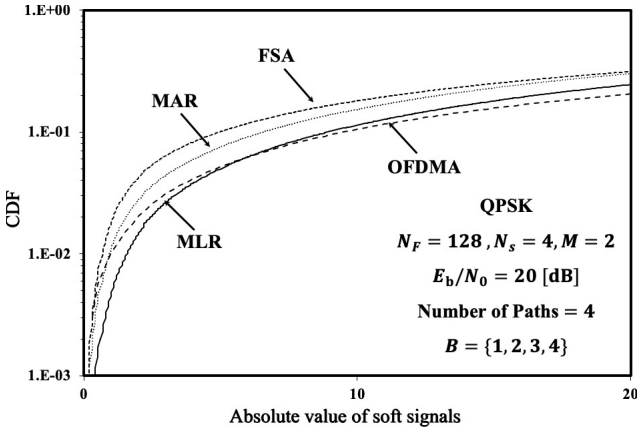

Fig. 7 CDF of absolute value of soft signals.

is allocated to every device. The lack of the diversity gain cause the small soft signals to appear with that probability. The MLR successfully reduces the probability to less than that of the other schemes, while the average absolute of the soft signal of the MLR is comparable to that of the OFDMA.

4.2 BER Performance

The BER performance of the proposed non-orthogonal multiple access is shown in Fig. 8, where the performances of the MLR is compared with the MAR. The performance of the FSA and the OFDMA are added as references in the figure. The channel model and the RB set are the same to those in the previous figures. As is expected from Fig. 7, the proposed non-orthogonal multiple access with the FSA achieves similar transmission performance as the OFDMA. Although the MAR attains better transmission performance than the FSA, the performance gap between them is only less than 1 dB at the BER of 10^{-4}. Although the MAR finds a subcarrier allocation index α that maximizes the average of the reliability as defined in (27), the MAR can only improve the reliability of the worst device a little bit. Since the BER performance is dominated by the worst device performance, the BER performance gap between the MAR and the FSA is only about 1 dB. On the other hand, the MLR achieves about 3 dB better transmission performance than the MAR at the BER of 10^{-4}. In a word, the MLR attains a gain of about 5 dB at the BER of 10^{-4} compared with the OFDMA.

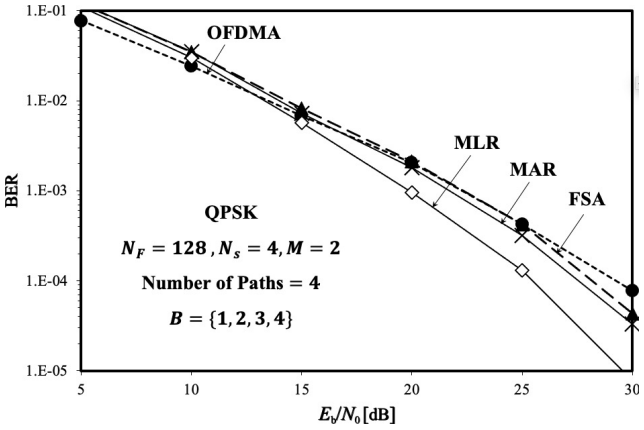

Fig. 8 BER performance of non-orthogonal multiple access.

4.3 Performance Analysis of MLR

Because it is revealed that the MLR is better than the MAR, the performance of the MLR is analyzed in the following. Figure 9 shows the reliability of the worst device $\Psi_\alpha(l_{\min})$ with the respect to the number of the paths in the channel. The performance of the FSA is added in the figure. The RB set is the same to that in the previous performance evaluation. The ordinate is the reliability of the worst device $\Psi_\alpha(l_{\min})$ at the CDF of 10^{-2}, and the abscissa is the number of the paths. The reliability is increased as the number of the paths increases. The gap between the two algorithm gets greater as the number of the paths increases. Figure 10 shows the reliability with respect to the RB set parameter. In this section, the RB set is defined as $B_k = \{1, 1+k, 1+2k, 1+3k\}$. Since the entries in the set can not exceed the highest frequency index, the subscript k ranges as $1 \le k \le \lceil \frac{N_F - 1}{3} \rceil$ where $\lceil \alpha \rceil$ is the maximum integer less than α. Since N_F is 128 in the simulation, the range can be written as $1 \le k \le 42$. The RBs can be indexed by the subscript k. While the ordinate

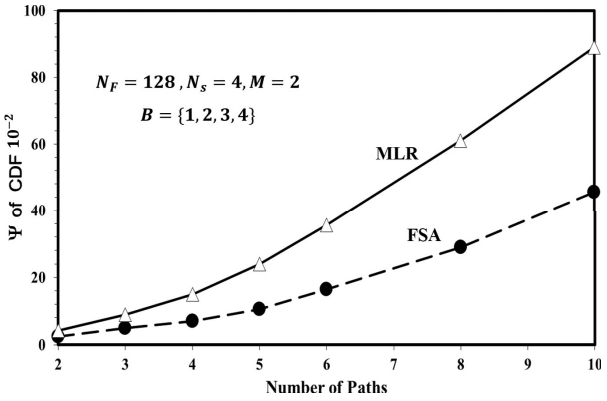

Fig. 9 Reliability $\Psi_\alpha(l_{\min})$ with respect to the number of paths.

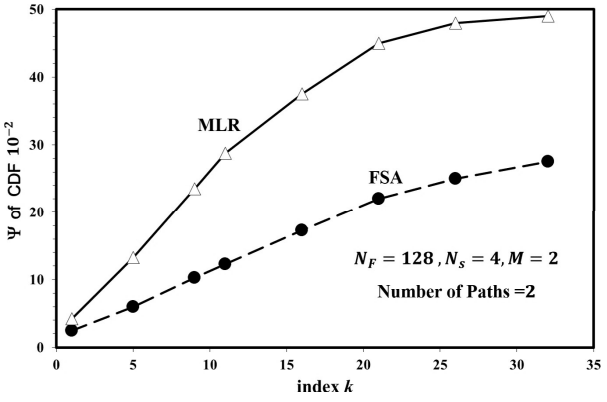

Fig. 10 Reliability $\Psi_\alpha(l_{\min})$ with respect to the RB set parameter.

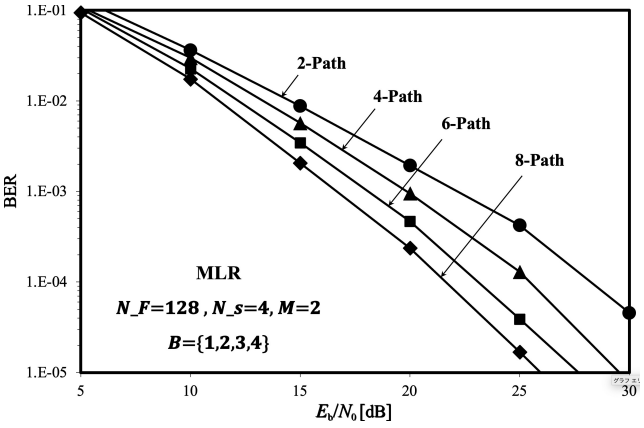

Fig. 11 BER performance with respect to number of paths.

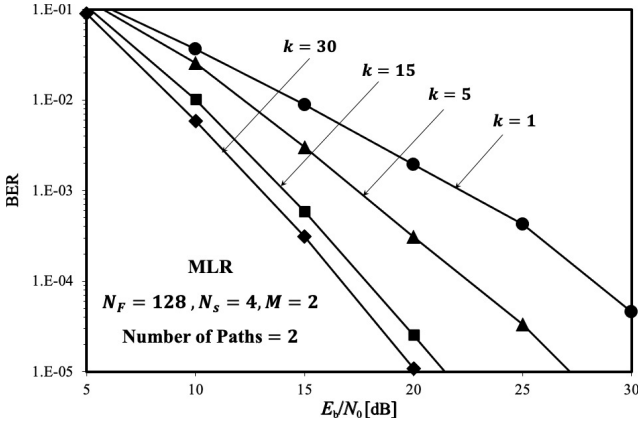

Fig. 12 BER performance with respect to the RB set.

of the figure is the reliability of the worst device $\Psi_\alpha(l_{\min})$ at the CDF of 10^{-2}, the abscissa is the index k. The number of paths is 2. As is well known, the transmission performance is improved as the diversity gain becomes higher in multicarrier systems with forward error correction such as OFDM. On the other hand, the relationship between Fig. 5, Fig. 6, and Fig. 8 proves that the reliability is regarded as a measure of the transmission performance in the proposed non-orthogonal access. This infers that the diversity gain is in proportion to the reliability in the proposed access. As the index k increases, the received signals become less correlated with each other. In other words, the increase in the index k makes the channels highly frequency selective, which is expected to give higher diversity gain to the proposed non-orthogonal access. As the number of the paths increases, also, the frequency selectivity becomes higher, which makes the proposed access achieve higher diversity gain. This leads that the increase in the index k or the number of the paths raises the reliability, because the diversity gain is proportional to the reliability as is described above. The reliability is increased as the index k gets bigger. The MLR increases the reliability much greater than the FSA as the index k become bigger.

The BER performance of the MLR v.s. the E_b/N_0 is shown in Fig. 11. When the RB set $B = \{1, 2, 3, 4\}$ is used, i.e., $k = 1$, as is expected, the BER performance is more improved as the number of the paths increases. Figure 12 shows the BER performance of the MLR with respect to the E_b/N_0, where 2-path Rayleigh fading is applied. In the figure, the performances with the RB set indexes of from 5 to 15 are drawn. Higher index enables the proposed adaptive subcarrier allocation to achieve better transmission performance. The adaptive subcarrier allocation based on the MLR with the index of 30 attains about 15 dB better transmission performance than that with the index of 1 at the BER of 10^{-5}.

5. Conclusions

This paper has proposed a non-orthogonal multiple access with adaptive subcarrier allocation. The proposed non-orthogonal multiple access assigns multiple frequency resources for each device to send their packets, even if the number of the devices exceeds that of the frequency resources. Furthermore, this paper has proposed adaptive subcarrier allocation based on factor graphs that adaptively allocates the frequency resources to the devices for improvement of the transmission performances. This paper has proposed two allocation algorithms for the proposed adaptive allocation. One of the two algorithm allocates the resources to the devices to maximize the reliability of the signals sent to the

device in the worst environment, which is named "MLR" in this paper. The other algorithm allocates the resource to the devices to maximize the average reliability of all the signals sent to the devices, which is named "MAR" in this paper.

Computer simulation confirms the performance of the proposed non-orthogonal multiple access. While the transmission performance of the proposed non-orthogonal access with the fixed subcarrier allocation is similar as that of the conventional OFDMA in 4-path fading channel, the proposed adaptive subcarrier allocation makes the proposed non-orthogonal access achieves better transmission performance than the OFDMA even though the transmission rate of the proposed non-orthogonal access is 1.5 times as high as the OFDMA, i.e., the overloading ratio of 1.5. While the MAR achieves a little bit better BER performance than the fixed subcarrier allocation, the MLR attains about 3 dB better BER performance than the MAR. Eventually, the MLR achieves a gain of about 5 dB at the BER of 10^{-4} compared the fixed allocation in the 4-path Rayleigh fading channel. Because the MLR achieves better transmission performance than the MAR, the characteristics of the MLR are analyzed. The MLR enables the proposed non-orthogonal multiple access to achieve a greater diversity gain as the number of the paths increases. The performance of the proposed non-orthogonal multiple access depends on the RB set parameters. The transmission performance is more improved as the frequency indexes in the set are widely distributed.

Acknowledgments

The work has been supported by JSPS KAKENHI JP21K04061 and the support center for advanced telecommunications technology research (SCAT).

References

[1] M. Ghosh, "A comparison of normalizations for ZF precoded MU-MIMO systems in multipath fading channels," IEEE Wireless Commun. Lett., vol.2, no.5, pp.515–518, Oct. 2013.
[2] R. Aggarwal, M. Assaad, C.E. Koksal, and P. Schniter, "Joint scheduling and resource allocation in the OFDMA downlink: Utility maximization under imperfect channel-state information," IEEE Trans. Signal Process., vol.59, no.11, pp.5589–5604, Nov. 2011.
[3] A. Li, A. Benjebbour, X. Chen, H. Jiang, and H. Kayama, "Uplink non-orthogonal multiple access (NOMA) with single-carrier frequency division multiple access (SC-FDMA) for 5G systems," IEICE Trans. Cummun., vol.E98-B, no.8, pp.1426–1435, Aug. 2015.
[4] A. Li, A. Benjebbour, K. Saito, Y. Kishiyama, and T. Nakamura, "Downlink non-orthogonal multiple access (NOMA) combined with single user MIMO (SU-MIMO)," IEICE Trans. Cummun., vol.E98-B, no.8, pp.1415–1425, Aug. 2015.
[5] Q. Luo, P. Gao, Z. Liu, L. Xiao, Z. Mheich, P. Xiao, and A. Maaref, "An error rate comparison of power domain non-orthogonal multiple access and sparse code multiple access," IEEE Open J. Commun. Soc., vol.2, pp.500–511, March 2021.
[6] R. Stoica, G. Abreu, Z. Liu, T. Hara, and K. Ishibashi, "Massively concurrent non-orthogonal multiple access for 5G networks and beyond," IEEE Access, vol.7, pp.82080–82100, June 2019.
[7] S.M.A. Kazmi, N.H. Tran, T.M. Ho, D. Niyato, and C.S. Hong, "Coordinated device-to-device communication with non-orthogonal multiple access in future wireless cellular networks," IEEE Access, vol.6, pp.39860–39875, June 2018.
[8] K. Higuchi and A. Benjebbour, "Non-orthogonal multiple access (NOMA) with successive interference cancellation for future radio access," IEICE Trans. Commun., vol.E98-B, no.3, pp.403–414, March 2015.
[9] Q. Liu, Q. Zhang, X. Xin, R. Gao, Q. Tian, and F. Tian, "Subchannel and power allocation with fairness guaranteed for the downlink of NOMA-based networks," IEICE Trans. Commun., vol.E103-B, no.12, pp.1447–1461, Dec. 2020.
[10] R. Hoshyar, F.P. Wathan, and R. Tafazolli, "Novel low-density signature for synchronous CDMA systems over AWGN channel," IEEE Trans. Signal Process., vol.56, no.4, pp.1616–1626, April 2008.
[11] E. Okamoto and M. Hoshino, "Non-orthogonal multiple access scheme suitable for machine type communication (MTC) and its applications," IEICE Trans. Commun. (Japanese edition), vol.J100-B, no.8, pp.505–519, 2017.
[12] C. Simon and T. Walingo, "Resource allocation for uplink SCMA NOMA in heterogeneous networks," IEEE AFRICON, 2019.
[13] W. Ahsan, W. Yi, Z. Qin, Y. Liu, and A. Nallanathan, "Resource allocation in uplink NOMA-IoT networks: A reinforcement-learning approach," IEEE Trans. Wireless Commun., vol.20, no.8, pp.5083–5098, 2021.
[14] V.H. Nikopour and H. Baligh, "Sparce code multiple access," Proc. IEEE Int'l Symp. Personal Indoor and Mobile Radio Communications (PIMRC), pp.332–336, Sept. 2013.
[15] X. Zhang, W. Ge, X. Wu, and W. Dai, "A low-complexity and fast convergence message passing receiver based on partial codeword transmission for SCMA systems," IEICE Trans. Commun., vol.E101-B, no.11, pp.2259–2266, Nov. 2018.
[16] R. Gallager, "Low-density parity-check codes," IRE Trans. Inf. Theory, vol.8-1, pp.21–28, Jan. 1962.
[17] R. Herzallah, "Probabilistic message passing for decentralized control of stochastic complex systems," IEEE Access, vol.7, pp.184707–184717, Dec. 2019.

Taichi Yamagami received the B.S. and M.S. degrees from Okayama University, Japan, in 2020 and 2022, respectively. He joined with Furukawa electric co., ltd. in 2022, His research interests include signal processing, wireless communication systems, and non-orthogonal multiple access.

Satoshi Denno received the M.E. and Ph.D. degrees from Kyoto University, Kyoto, Japan in 1988 and 2000, respectively. He joined NTT radio communications systems labs, Yokosuka, Japan, in 1988. He was seconded to ATR adaptive communications research laboratories, Kyoto, Japan in 1997. From 2000 to 2002, he worked for NTT DOCOMO, Yokosuka, Japan. In 2002, he moved to DOCOMO communications laboratories Europe GmbH, Germany. From 2004 to 2011, he worked as an associate professor at Kyoto University. Since 2011, he is a full professor at graduate school of natural science and technology, Okayama University. From the beginning of his research career, he has been engaged in the research and development of digital mobile radio communications. In particular, he has considerable interests in channel equalization, array signal processing, Space time codes, spatial multiplexing, and multimode reception. He won the Best paper award of the 19th international symposium on wireless personal multimedia communications (WPMC2016), and the outstanding paper award of the 23rd international conference on advanced communications technology (ICAT2021). He received the excellent paper award from the IEICE and the best paper award from the IEICE communication society in 1995 and 2020, respectively.

Yafei Hou received his Ph.D. degrees from Fudan University, China and Kochi University of Technology (KUT), Japan in 2007. He was a post-doctoral research fellow at Ryukoku University, Japan from August 2007 to September 2010. He was a research scientist at Wave Engineering Laboratories, ATR Institute International, Japan from October 2010 to March 2014. He was an Assistant Professor at the Graduate School of Information Science, Nara Institute of Science and Technology, Japan from April 2014 to March 2017. He became an assistant professor at the Graduate School of Natural Science and Technology, Okayama University, Japan from April 2017. He is a guest research scientist at Wave Engineering Laboratories, ATR Institute International, Japan from October 2016. His research interest are communication systems, wireless networks, and signal processing. He received IEICE (the Institute of Electronics, Information and Communication Engineers) Communications Society Best Paper Award in 2016, 2020, and Best Tutorial Paper Award in 2017. Dr. Hou is a senior member of the IEEE and a member of the IEICE.